Lean Meat Yield estimation using a prototype 3D Imaging approach

Alen Alempijevic[a,*], Teresa Vidal-Calleja[a], Raphael Falque[a], Phillip Quin[a], Edwina Toohey[d], Brad Walmsley[c], Malcolm McPhee[b]

[a] *Center for Autonomous Systems, University of Technology Sydney, P.O. Box 123, Broadway, NSW 2007, Australia*
[b] *NSW Department of Primary Industries, Livestock Industries Centre, Armidale, NSW 2351, Australia*
[c] *NSW Department of Primary Industries, Animal Genetics and Breeding Unit (AGBU[†]), Armidale, NSW 2351, Australia*
[d] *NSW Department of Primary Industries, Centre for Sheep Meat Development, P.O. Box 129, Cowra, NSW 2794, Australia*

Abstract

Lean Meat Yield (LMY, %) of carcass is an important industry trait, which currently is not routinely measured in Australian beef abattoirs. Objective on-line technology to determine LMY is key for wider adoption. This paper presents a proof-of-concept approach for estimating the LMY of beef carcasses from the 3D information provided by RGB-D cameras. Moreover, a specifically designed on-line data acquisition system for abattoir applications is presented, consisting of three cameras moving on a scanning rig to generate 3D carcass side reconstructions. The hindquarter is then segmented consistently across all the 3D models to extract curvature information and LMY estimated via non-linear regression based on Gaussian Process models. Sides from 119 carcasses at two different commercial abattoirs were used to evaluate this approach. Results from this preliminary study (RMSE=3.91%, R^2=0.69) using curvature, P8 fat

*Corresponding author
Email addresses: alen.alempijevic@uts.edu.au (Alen Alempijevic), teresa.vidalcalleja@uts.edu.au (Teresa Vidal-Calleja), raphael.guenot-falque@uts.edu.au (Raphael Falque), phillip.quin@uts.edu.au (Phillip Quin), edwina.toohey@dpi.nsw.gov.au (Edwina Toohey), brad.walmsley@dpi.nsw.gov.au (Brad Walmsley), malcolm.mcphee@dpi.nsw.gov.au (Malcolm McPhee)

[†]AGBU is a joint venture of NSW Department of Primary Industries and University of New England

and HSCW indicate that 3D imaging of beef carcasses is a viable and relatively accurate technology to estimate LMY.

Keywords: Lean Meat Yield, Beef, Carcass Grading, Computer Vision

---

1. Introduction

Weight and fatness are key contributors to the profitability in the Australian beef value chain. There is a movement towards payment systems that more accurately reflect what has been produced in terms of quality such as Meat Standards Australia (MSA) eating quality (Watson et al., 2008) and more recently MSA index (McGilchrist et al., 2019) and quantity (lean meat yield LMY, %). This movement has prompted the industry to invest in technologies to accurately measure this.

In order to commercially determine LMY, extensive research has been conducted over the past few decades in Australia and around the world into the development of objective online measurement technologies, e.g. (Craigie et al., 2012; Hopkins et al., 2004). The research and development of these technologies has largely been driven by the need to satisfy consumer demands for quality, provide more accurate carcass feedback to producers and reduce labour requirements for processors (Hopkins et al., 2004).

Computed Tomography (CT) has been used to determine carcass lean and fat components (Kongsro et al., 2009) with a high degree of accuracy and is considered the gold standard. Currently, within Australia there is no industry-accepted method for predicting LMY of beef carcasses (Biddle et al., 2016). Stemming from the need to objectively assess LMY, alternative commercial methods have been developed.

Video Image Analysis (VIA) is one of the most widely researched non-destructive, non-invasive technologies which looks at carcasses assessment (Rius-Vilarrasa et al., 2009). Initial VIA technology evaluated Hot Standard Carcass Weight (HSCW) by capturing 2D images of the lateral view of carcasses or sides. From these images, colour (red, blue, green scale) and dimensional data

are extracted to estimate yield, conformation and EUROP fat and conformation scores (Borggaard et al., 1996; Allen, 2009). More recently VIA systems use striping or structured light to create full 3D reconstructions (Craigie et al., 2013). Based on the scientific literature it would appear that the whole beef body VIA technology is useful for evaluating beef carcass composition. The published data on VIA technology has been used to estimate Saleable Meat Yield (SMY) of whole carcasses (Craigie et al., 2013) or on a per cut basis (Pabiou et al., 2011) where SMY is defined as the saleable product including muscle, fat and bone. In line with Australian research objectives (Biddle et al., 2016) LMY is a universal measure irrespective of abattoir and market specification, and can be a consistent feedback mechanism to producers subject to the availability of suitable LMY measurement technologies.

Recently, technologies based on Dual Energy X-Ray Absorptiometry (DEXA) (Gardner et al., 2018) have been developed and evaluated. This study reports on the development of a prototype 3D imaging approach that is a low-cost technology alternative to the DEXA technology. Information about the internal properties of a carcass such as fat and muscle composition cannot be directly ascertained from a view of the outer surface. However, the size of muscles, and the presence of more or less fat, affect the curvature of the outer surface. The curvature of the surface of a carcass is therefore expected to be correlated to muscle and fat proportions. The automation of the feature extraction related to LMY (e.g., local curvature or volume information) is then a challenging task (Van Kaick et al., 2011), as it requires a consistent annotation of beef carcass shapes that are slightly different in terms of the shape, rotation, scale, and colour.

In this paper, we introduce a system capable of densely reconstructing the shape of 3D carcasses using low cost red green blue and depth (RGB-D) cameras. A method to consistently extract 3D descriptors from the dense reconstructions is presented. We demonstrate correlation between a curvature descriptor from the segmented 3D region and LMY.

2. Materials and Methods

2.1. Animals, experimental design, treatments and sample collection

This study was conducted using carcass sides from 119 cows, steers, and heifers across a range of breeds at two abattoirs. Summary statistics for P8 fat depth, HSCW, and LMY (CT Lean (kg) / HSCW (kg) expressed in %) at each abattoir are reported in Table 1 and the distribution of LMY is provided in Figure 1. Carcass sides averaged 2.5 meters in length and were scanned with RGB-D cameras between 30 mins and 20 hours post-mortem.

Abattoir A

Ninety-three Angus carcass sides were scanned as part of 3 slaughters (separated by several months) by an operator using a hand-held prototype device and open source software (Newcombe et al., 2011). Only the interior surface of the beef side was scanned, from leg through rib cage, the external surface was not acquired. The left-hand side of each carcass was processed with fat trimming limited to only that required for hygiene purposes and kidney fat retained in the side. A MSA trade development officer using MSA protocols (Watson et al., 2008) graded all carcasses. After grading the left-hand side of the carcass was boned-out to determine beef primal cut, fat trim and bone weights (Perry et al., 2001). The untrimmed boneless primals were transported to the University of New England (UNE), Armidale, NSW and scanned using a Picker Ultra Z Spiral CT-scanner (Philips Medical Imaging Australia, Sydney NSW). The spiral abdomen protocol was selected with the following settings: pilot scan length of 512 mm, field of view set at 480mm, Index 20, kV 110, mA 150, revs 40, pitch 1.5 and standard algorithm. Image analysis software (Laurenson et al., 2013) was used to estimate lean and fat tissue weights (kg) from scanned images. The CT scanned lean and fat tissue weights were adjusted to untrimmed boneless primal weights, to correct for differences between CT predicted weights and scale measured untrimmed weights.

Abattoir B

Twenty-six carcass sides were scanned using a rig as described in Section 2.3.

The carcass sides scanned at abattoir B were part of a larger study that comprised 60 head used to evaluate the DEXA technology (Gardner et al., 2018), where the scanning activity was conducted, on site, over two consecutive weeks. All carcass sides were conventionally chilled for 24 hours before being processed into smaller pieces for CT scanning. The cold weight of each quarter was measured shortly after removal from the chiller. Forequarters were cut into 9 smaller primal sections while hindquarters were cut into 7 sections. Each beef carcass side was therefore CT scanned in a total of 16 sections, allowing all components to fit within the 500mm x 500mm CT aperture. The cutting lines used to cut each carcass side into 16 sections were based on the abattoir commercial cutting lines to enable subsequent dissection into saleable cuts of meat. The two sides of each carcass (spray-chilled and non-spray chilled sections) were CT scanned consecutively. CT image analysis was done according to the method described by Anderson et al. (2015).

2.2. Approach Overview

The approach presented in this paper reconstructs a 3D model of the carcass side from red green blue and depth (RGB-D) images. A scanning rig has been designed specifically for the collection of the images in order to contribute towards online deployments in abattoirs. This rig is equipped with multiple moving RGB-D cameras which capture a large number of overlapping frames of the carcass side. These individual frames are then fused together to create a single reconstruction of the carcass side 3D shape. Once the 3D reconstruction is completed, a coarse-to-fine method is used to segment accurately a region of the 3D carcass side by transferring the annotation of a manually annotated template onto the carcass side reconstruction. Thereafter, curvature information of this region is extracted and parameterised into a histogram. These feature descriptors are inputs to a non-linear regression algorithm, Gaussian Process (Rasmussen & Williams, 2006), a supervised learning approach which is trained to estimate LMY of the carcass side's 3D models against CT LMY (as a percentage of HSCW). A flowchart of the methodology is shown in Figure 2.

2.3. Data Collection Rig

The RGB-D images of the carcass sides are collected using the bespoke rig shown in Figure 3. Three vertical beams are spaced 120 degrees apart, forming a circle around a rotating base wide enough to fit a beef carcass side. Each vertical strut supports a rail and belt system on which a Primesense Carmine v1.09 RGB-D sensor is mounted, such that it can move vertically.

During scanning, the Achilles tendon suspended carcass side, is manually moved along the rail into the centre of the rig. This process would be automated in a commercial ready product. The cameras move vertically as the base rotates 180° through discrete positions, acquiring a set of vertical strips of imagery which cover the carcass side from all angles other than from directly above and below. The motion of the rig is illustrated in Figure 4. The 180° rotation allows the carcass side to continue along the rail after scanning.

The RGB-D cameras, rig control and logging of data are all performed on a single unit of computing, Intel NUC Skull Canyon product running Ubuntu 16.04. The software framework leverages the Robotic Operating System (ROS Kinetic Kame) (Quigley et al., 2009) which contains drivers for the cameras and motors as well as utilities for logging data. University of Technology Sydney - Centre for Autonomous Systems, have developed the additional code for controlling the rig, cameras and subsequent processing of data in C++ running as nodes in the ROS framework.

2.4. 3D Reconstruction

The method for 3D reconstruction used in this work takes a series of RGB and depth images as inputs, referred to as a frame, and generates a 3D point-cloud of a carcass side segmented from the background. Visual features with depth information are extracted from each RGB-D image to recover 3D points on the carcass side. Correspondences between frames are found through visual descriptors (Lowe, 2004). These correspondences are used to find the relative transformation between frames. Given the relative transformations of the consecutive and non-consecutive frames and across cameras, an optimisation algo-

rithm (Kummerle et al., 2011) is used to obtain the camera trajectories (i.e., position and orientation of the three cameras over time).

The reconstructed pointcloud can then be generated from the RGB-D data associated with each frame. Finally, a Poisson mesh reconstruction (Kazhdan & Hoppe, 2013) is run over the reconstructed pointcloud to create a closed surface mesh. Figure 5 shows a few sample reconstructed models.

2.5. Consistent curvature description

The curvature description used as input to the machine learning-based regression algorithm, needs to be consistent across all the scanned carcasses, especially when focused only in individual muscle groups. The region of interest is shown in red in Figure 6. In this approach, the consistency problem is solved by annotating one of the scanned 3D shapes, referred to as the annotated template, and morphing this 3D shape onto all the other 3D scanned carcass sides, referred to as targets to segment the region of interest. After morphing, the annotation is then transferred onto all the targets and used to compute the curvature descriptors.

2.5.1. Consistent segmentation

The method to achieve a consistent segmentation of the region of interest employs a semi-automatic coarse-to-fine approach, where the coarse alignment is provided using manual annotations while the refinement step is performed automatically.

The morphing approach is based on non-rigid deformation (Sumner et al., 2007) using initially a set of corresponding sparse points to deform non-rigidly the template by minimising the distance between these points, while maximising rigidity and finally refining with dense correspondences. Once the annotated template is finely aligned with the target, the annotation is transferred onto the target by finding the closest points from template to the target and copying the annotation. Given these annotations for all carcass sides, a curvature descriptor can be consistently obtained over the segmented region of interest. An

example of the consistent segmentation is shown in Figure 6.

2.5.2. Curvature descriptor

The approach to encoding curvature exploited in this work leverages Darboux frames defined at each point of the hindquarter and the viewpoint defined at the centre of the hook (Rusu et al., 2010), which anatomically correlates to the Achilles tendon. For a pair of 3D points $\mathbf{p}_i$, $\mathbf{p}_j \in \mathbb{R}^3$, a Darboux frame is defined in $\mathbf{p}_i$, with axis presented in Figure 7 and vectors:

$$\begin{aligned} \mathbf{u} &= \mathbf{n}_i \\ \mathbf{v} &= \mathbf{u} \times \frac{\mathbf{p}_j - \mathbf{p}_i}{d} \\ \mathbf{w} &= \mathbf{u} \times \mathbf{v} \end{aligned} \tag{1}$$

Using the defined Darboux frame, three angular features α, ϕ and θ (which are scalars and are annotated in Figure 7) are computed between surface normals $\mathbf{u}$, $\mathbf{v}$, $\mathbf{w}$ and $\mathbf{n}_j$. The cosine of the angle between two vectors is equal to the dot product of these vectors divided by the product of vector magnitude, for example

$$\mathbf{cos}\alpha = \frac{\mathbf{n}_j \mathbf{v}}{|\mathbf{n}_j||\mathbf{v}|} \tag{2}$$

The final representation of the curvature descriptor is created by binning α, ϕ and θ into a histogram. This histogram of these orientations between pairs of surface normals is referred to as a curvature descriptor.

2.5.3. Volumetric Descriptor

As an alternative to curvature descriptors, we extract volumetric information computed using a morphed annotated template as shown in Figure 8. The volume computation is obtained from the 3d mesh by partitioning the space into a set of tethraedra. For each triangle in the mesh, a tetrahedron is generated using the points from the triangle and the mesh centroid. The mesh volume is

then obtained by integrating the sum of the signed volume of each tetrahedron. We aggregate all volumes extracted from the morphed annotated template into a signature.

2.6. Statistical Analysis

2.6.1. Non-linear regression for lean meat yield estimation

Gaussian Process (GP) model (Rasmussen & Williams, 2006) is a widely used approach for non-linear probabilistic regression that can be seen as a distribution over functions. Given a set of training examples with ground truth information, a mean function, and a kernel function, this model aims to find the distribution that best fits the training set using maximum likelihood estimation.

A GP model, with a zero-mean function and a Matérn kernel, was trained in a supervised manner using as input the curvature descriptor, and optionally other independent variables such as HSCW or P8, and as output the ground truth of LMY. The Matérn kernel defines the covariance between two input points at distance l from each other as:

$$C_\nu = \sigma^2 \frac{2^{1-\nu}}{\Gamma(\nu)} \left(\sqrt{2\omega} \frac{l}{\rho} \right)^{\omega} K_\nu \left(\sqrt{2\nu} \frac{l}{\rho} \right) \tag{3}$$

where Γ is the gamma function, K_ω is the modified Bessel function of the second kind of order ν, ρ is the characteristic length scale, and ν controls the smoothness of the final function after the covariance function has been applied.

2.6.2. Ten-fold cross validation

A 10-fold cross validation procedure was used (Refaeilzadeh et al., 2009). Data from all datasets was combined, and split into 90% training, 10% testing (10-fold cross validation). Given the trained GP regression model, an unseen carcass LMY value can be estimated by inputting a carcass side's curvature descriptor to the GP model. The root mean square error (RMSE) along with the coefficient of determination (R^2) are reported.

2.6.3. Genetic Algorithm

Feature selection (reduction), is the process of finding the most relevant inputs for a model. We undertake feature selection via a Genetic Algorithm (GA) (Whitley, 1994). The GA is configured to search the curvature descriptor space to select a subset of features that estimate LMY with the lowest RMSE. This analysis is a parameter search, which in turn requires partitioning a set of validation data from the training data used in optimisation. It is performed using a hold out of data (representative of the probability distribution of the entire dataset with respect to LMY).

3. Results

The ablation study of the proposed method considering both, linear regression and the Gaussian process regression model is given in Table 2 and Table 3, respectively. This study examines the cases of the curvature descriptor depicted in Section 2.5.2 computed with and without consistent segmentation[2] of the region of interest and the concatenation of the curvature descriptor with two independent measurements: P8 fat depth and HSCW.

While the information provided by the P8 fat depth and the HSCW is insufficient to estimate LMY, they provide a significant improvement of performance when combined with the curvature descriptor as shown in Table 3. One of the key points highlighted by these results is how a consistent segmentation of the carcass side shape significantly improves the prediction performance of the GP.

The possibility of reducing the dimensionality of curvature descriptor with respect to their capability to describe LMY is evaluated via a GA. The GA is configured to search the curvature descriptor space to select a subset of 30 features that estimate LMY with the lowest RMSE. This analysis is performed using a hold out of 10% of data which is used for validation, and with 90% for

[2]Segmentation by height corresponds to cropping the carcass side at a constant distance from the highest point to extract the region of interest.

training the GA model. These results are noted with a (*) in Table 2 and 3, as they are not performed across 10 random folds, rather a hold-out of a single representative fold of data.

Finally for comparison, the curvature descriptor is compared to a volumetric based feature descriptor on the task of LMY prediction. This volumetric descriptor and the curvature descriptor using the consistent segmentation have been extracted on the dataset from Abattoir B. The dataset from Abattoir A using hand-held scanner device only has scans of the inner part of the carcass sides and could not be used for the volume computations. The results of a regression using a Gaussian Process on all the different feature descriptors is provided in Table 4. As shown in the table, the curvature descriptor using the consistent segmentation outperforms the volume based feature descriptors with a lower RMSE and higher R^2 . This is emphasized by the high-dimensionality of the curvature descriptor making it more difficult to be trained on smaller datasets.

4. Discussion

This preliminary study has demonstrated that it is feasible to densely reconstruct the shape of a 3D carcass using low cost RGB-D cameras to estimate LMY (RMSE=4.34%, R^2=0.62) between measured CT LMY and estimates of LMY (Figure 9). Figure 9a indicates that there was no bias in the slope and that the residuals in Figure 9b show that most carcasses lie within $\pm$ 5%.

Using the curvature descriptor trained via a Gaussian process, the LMY as a percentage of total HSCW was successfully estimated from RGB-D images of the exterior of the carcass side. Linear regression models are not flexible enough to handle the complexity of the problem at hand, as shown in Table 2. A Gaussian process model performs better in this case as it suitable for non-linear regression problems and can handle high dimensional feature vectors as shown in Table 3.

Combining the curvature descriptor with the P8 fat depth and HSCW re-

sulted in RMSE =3.91% and R^2=0.69, indicating that fatness and HSCW provide independent observations to curvature, and assist in estimating LMY. Dimensionality reduction to select elements of curvature descriptor that are more related to LMY further enhances the estimation capability RMSE=3.73%, R^2=0.74. However, additional data is required to evaluate. As a comparison, preliminary results reported on DEXA (Gardner et al., 2018) on predicting CT Fat %, on dataset B used in this paper, showed RMSE=3.2% and R^2=0.88.

Currently, to the authors knowledge, there have not been any reported studies on estimating LMY for beef carcasses using either 2D or 3D cameras. However, there are several studies and commercial companies with products in estimating SMY, conformation and EUROP fat and conformation scores (Borggaard et al., 1996; Craigie et al., 2013; Pabiou et al., 2011). While SMY relates to weight and by virtue volume, LMY represents the quantity of solely muscle as a component of the volume.

To indicate the capacity of volume in estimating LMY, a subset of data (n=27) was used. The 3D carcass sides were processed using the proposed morphing approach, thereby extracting consistent volumes across all carcasses. The capacity of volume to estimate LMY was very low R^2=0.07. Caution needs to be applied due to the low number of samples and revisited with additional data.

Under commercial abattoir processing operations, the carcass side needs to be 3D scanned within 30-60 seconds to keep up with chain speed (Toohey et al., 2018) and avoid creating a bottleneck on entry to chillers. As a result of these constraints, approaches such as the hand-held scanner employed in collecting Abattoir A in this study are not commercially viable even though they result in high quality 3D models. Scanning manually took at least 30 minutes per carcass side, required manual intervention, as well as an additional operator to keep the carcass side from swinging.

The rig with three cameras, having motion around the carcass side, obtains over 5000 distinctively different camera views (i.e., camera poses). This is equivalent of having 5000 cameras distributed around the carcass side. The system

can handle a swinging carcass side, in this preliminary study the acquisition time was in order of 3-5 minutes. The acquisition time was a conservative approach for experimental purposes to ensure completeness of the 3D model given the limited number (n=119) of CT data to train the system. Improvements to the software process are aiming to reduce the scanning time, whereas the approach to estimate LMY is agnostic to source high quality 3D reconstruction (e.g., dense and noise-free meshes) of the surface of the carcass side.

Finally, the current rig occupies a footprint of radius 1.7m and operation is completely safe for humans and carcasses. The rig has been tested by acquisition in two chiller rooms at abattoirs reported in this study, and an additional abattoir where n=19 and CT data across the whole side was not collected.

5. Conclusion

Even though the results presented here are preliminary and use a prototype rig set up, the outcomes indicate that further work using 3D technology to estimate LMY is warranted. This preliminary work demonstrated that the proposed approach can estimate LMY (compared with CT LMY, RMSE=3.91% R^2=0.69). This technology can provide a cost-effective approach to evaluate LMY with minimal barriers to adoption (e.g., footprint). More data covering the full range of LMY and further comparisons with other technologies is needed to demonstrate the full capability of the technology described in this work.

Acknowledgment

The authors would like to extend our thanks to the commercial abattoirs for their support during the data collection phase and acknowledge that this work would not be possible without their continued support. We extend our thanks to JBS staff (Graham Treffone, Mark Kelly, Darrel Cody), TEYS Wagga Wagga staff (Grant Garey, Jasmine Nixon), Murdoch Team (Graham Gardner, Jarno, Chris Smith, C.J), Scott Automation Team (Jonathan Cook, Victor

Martchenko, Paul Danelutti), NSW DPI (Dan Ebert, Reg Woodgate, Jason Siddell) for the data obtained at serial slaughters across the abattoirs.

References

Allen, P. (2009). 20 - Automated grading of beef carcasses. In J. P. K. Ledward, & David (Eds.), *Improving the Sensory and Nutritional Quality of Fresh Meat* (pp. 479–492). Woodhead Publishing.

Anderson, F., Pannier, L., Pethick, D., & Gardner, G. (2015). Intramuscular fat in lamb muscle and the impact of selection for improved carcass lean meat yield. *Animal*, *9*, 1081–1090.

Biddle, R., Pattinson, R., Philpott, J., Polkinghorne, R., Thompson, J., Troja, P., & Williams, S. (2016). *Australian Beef Language 'White paper'*. `https://www.mla.com.au/Research-and-development/Search-RD-reports/RD-report-details/Market-Information/Australian-Beef-Language-White-Paper/3086`. Accessed December 15, 2020.

Borggaard, C., Madsen, N. T., & Thodberg, H. H. (1996). In-line image analysis in the slaughter industry, illustrated by beef carcass classification. *Meat Science*, *43*, 151–163.

Craigie, C. R., Navajas, E. A., Purchas, R. W., Maltin, C. A., Bunger, L., Hoskin, S. O., Ross, D. W., Morris, S. T., & Roehe, R. (2012). A review of the development and use of video image analysis (VIA) for beef carcass evaluation as an alternative to the current EUROP system and other subjective systems. *Meat Science*, *92*, 307–318.

Craigie, C. R., Ross, D. W., Maltin, C. A., Purchas, R. W., & Bunger, L. (2013). The relationship between video image analysis (via), visual classification, and saleable meat yield of sirloin and fillet cuts of beef carcasses differing in breed and gender. *Livestock Science*, *158*, 169–178.

Gardner, G., Starling, S., Charnley, J., Hocking-Edwards, J., Peterse, J., & Williams, A. (2018). Calibration of an on-line dual energy x-ray absorptiometer for estimating carcase composition in lamb at abattoir chain-speed. *Meat Science*, *144*, 91 – 99.

Hopkins, D., Safari, E., Thompson, J., & Smith, C. (2004). Video image analysis in the australian meat industry – precision and accuracy of predicting lean meat yield in lamb carcasses. *Meat Science*, *67*, 269–274.

Kazhdan, M., & Hoppe, H. (2013). Screened poisson surface reconstruction. *ACM Transactions on Graphics (ToG)*, *32*, 1–13.

Kongsro, J., Roe, M., Kvaal, K., Aastveit, A., & Egelandsdal, B. (2009). Prediction of fat, muscle and value in Norwegian lamb carcasses using EUROP classification, carcass shape and length measurements, visible light reflectance and computer tomography (CT). *Meat Science*, *1*, 102–107.

Kummerle, R., Grisetti, G., Strasdat, H., Konolige, K., & Burgard, W. (2011). G2o: A general framework for graph optimization. In *IEEE International Conference on Robotics and Automation (ICRA)* (pp. 3607–3613). IEEE. Shanghai, China.

Laurenson, Y., Walmsley, B., Oddy, V., Greenwood, P., & McPhee, M. (2013). Modelling trimmed fat from commercial primal cuts. In *Proceedings of the 20th International Congress on Modelling and Simulation* (pp. 1–6). Adelaide, Australia.

Lowe, D. G. (2004). Distinctive image features from scale-invariant keypoints. *International journal of computer vision*, *60*, 91–110.

McGilchrist, P., Polkinghorne, R., Ball, A., & Thompson, J. (2019). The meat standards australia index indicates beef carcass quality. *Animal*, *13*, 1750–1757.

Newcombe, R. A., Izadi, S., Hilliges, O., Molyneaux, D., Kim, D., Davison, A. J., Kohi, P., Shotton, J., Hodges, S., & Fitzgibbon, A. (2011). Kinectfusion:

Real-time dense surface mapping and tracking. In *Mixed and augmented reality (ISMAR), 2011 10th IEEE international symposium on* (pp. 127–136). Basel, Switzerland, IEEE.

Pabiou, T., Fikse, W. F., Cromie, A. R., Keane, M. G., Nasholm, A., & Berry, D. P. (2011). Use of digital images to predict carcass cut yields in cattle. *Livestock Science*, *137*, 130–140.

Perry, D., Shorthose, W., Ferguson, D., & Thompson, J. (2001). Methods used in the crc program for the determination of carcass yield and beef quality. *Australian Journal of Experimental Agriculture*, *41*, 953–957.

Quigley, M., Conley, K., Gerkey, B., Faust, J., Foote, T., Leibs, J., Wheeler, R., & Ng, A. Y. (2009). ROS: an open-source Robot Operating System. In *ICRA workshop on open source software* (pp. 1–5). Kobe, Japan volume 3.

Rasmussen, C. E., & Williams, C. K. (2006). *Gaussian processes for machine learning* volume 1. MIT press Cambridge.

Refaeilzadeh, P., Tang, L., & Liu, H. (2009). *Cross-Validation*. Boston, MA: Springer US. doi:10.1007/978-0-387-39940-9_565.

Rius-Vilarrasa, E., Bünger, L., Maltin, C., Matthews, K., & Roehe, R. (2009). Evaluation of Video Image Analysis (VIA) technology to predict meat yield of sheep carcasses on-line under UK abattoir conditions. *Meat Science*, *82*, 94–100.

Rusu, R. B., Bradski, G., Thibaux, R., & Hsu, J. (2010). Fast 3d recognition and pose using the viewpoint feature histogram. In *2010 IEEE/RSJ International Conference on Intelligent Robots and Systems* (pp. 2155–2162). Taipei, Taiwan, IEEE.

Sumner, R. W., Schmid, J., & Pauly, M. (2007). Embedded deformation for shape manipulation. *ACM Transactions on Graphics (ToG)*, *26*, 80–es.

Toohey, E., van de Ven, R., & Hopkins, D. (2018). The value of objective online measurement technology: Australian red meat processor perspective. *Animal Production Science*, *58*, 1559–1565.

Van Kaick, O., Zhang, H., Hamarneh, G., & Cohen-Or, D. (2011). A survey on shape correspondence. In *Computer Graphics Forum* (pp. 1681–1707). Wiley Online Library volume 30.

Watson, R., Gee, A., Polkinghorne, R., & Porter, M. (2008). Consumer assessment of eating quality–development of protocols for Meat Standards Australia (MSA) testing. *Australian Journal of Experimental Agriculture*, *48*, 1360–1367.

Whitley, D. (1994). A genetic algorithm tutorial. *Statistics and computing*, *4*, 65–85.

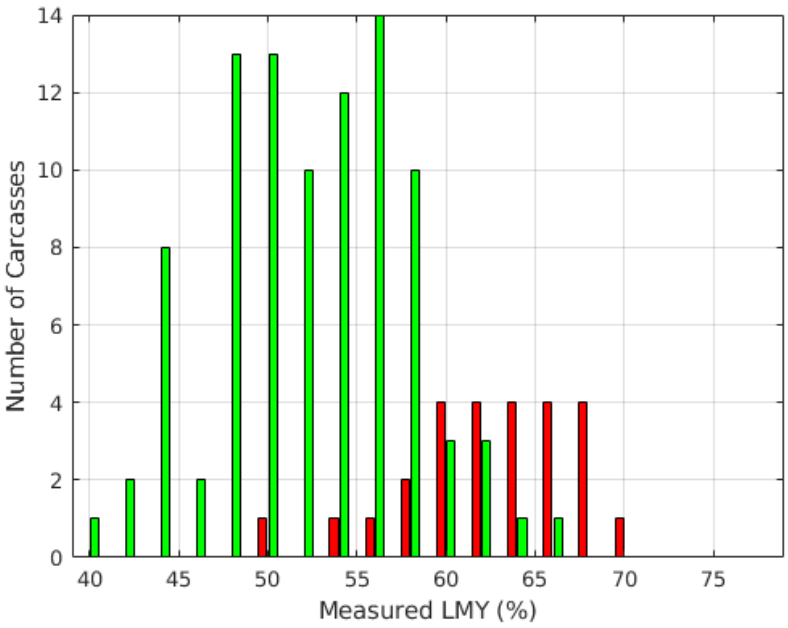

Figure 1: Number of carcasses with computed tomography lean meat yield (LMY, %) values at one unit intervals data for Abattoir A (green) and Abattoir B (red).

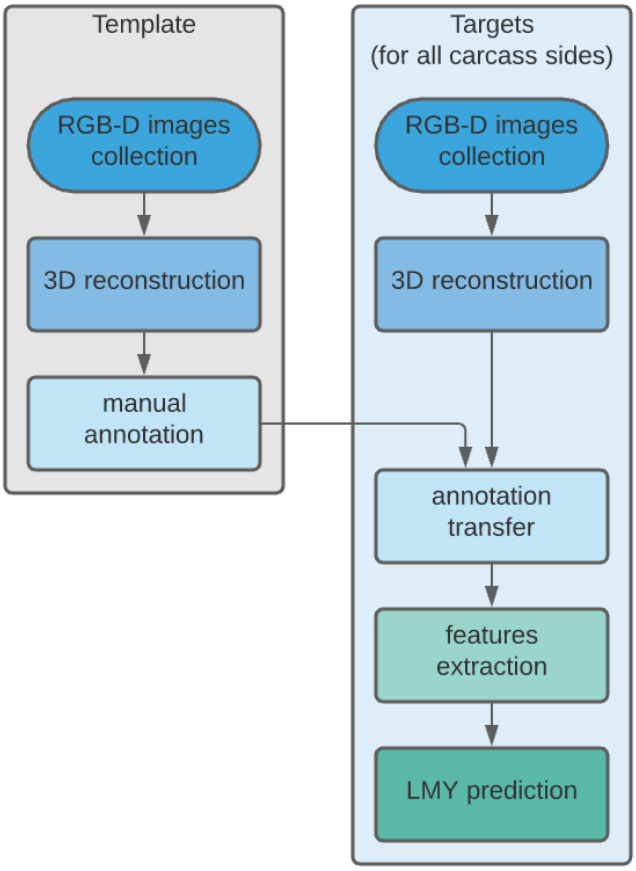

Figure 2: Flowchart of the methodology proposed in this approach of using red green blue and depth (RGB-D) images to develop 3 Dimensional (3D) reconstructions and subsequently estimate lean meat yield (LMY, %).

Figure 3: A beef carcass side being scanned by the custom-built rig.

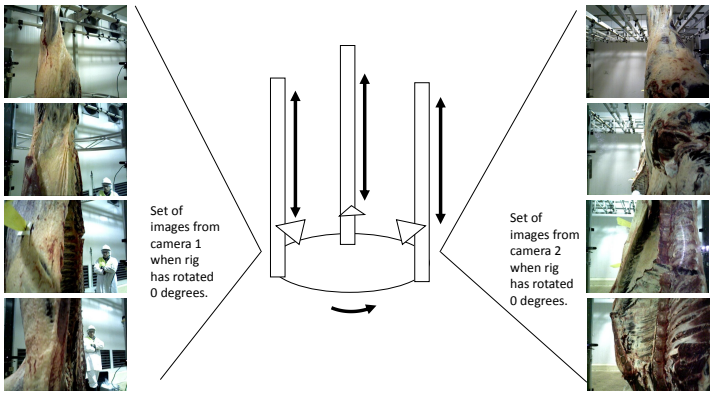

Figure 4: The rig and camera configuration. Arrows show the possible motion of the three cameras and the rotation of the rig assembly around the base. On the left and right are example RGB images captured by the RGB-D cameras during the scanning of a beef carcass side.

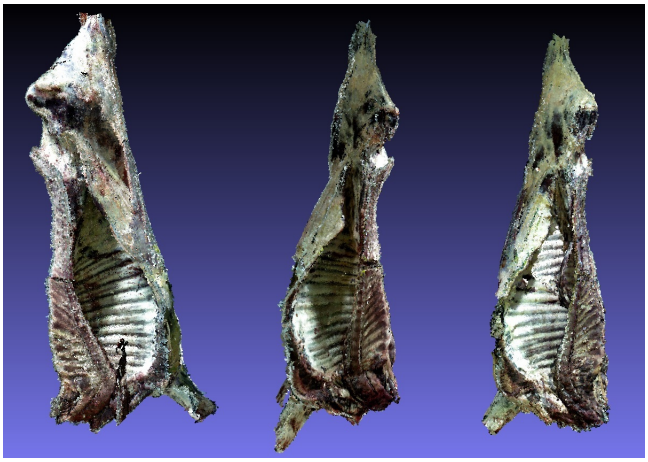

Figure 5: Reconstructed 3D models of beef carcass sides.

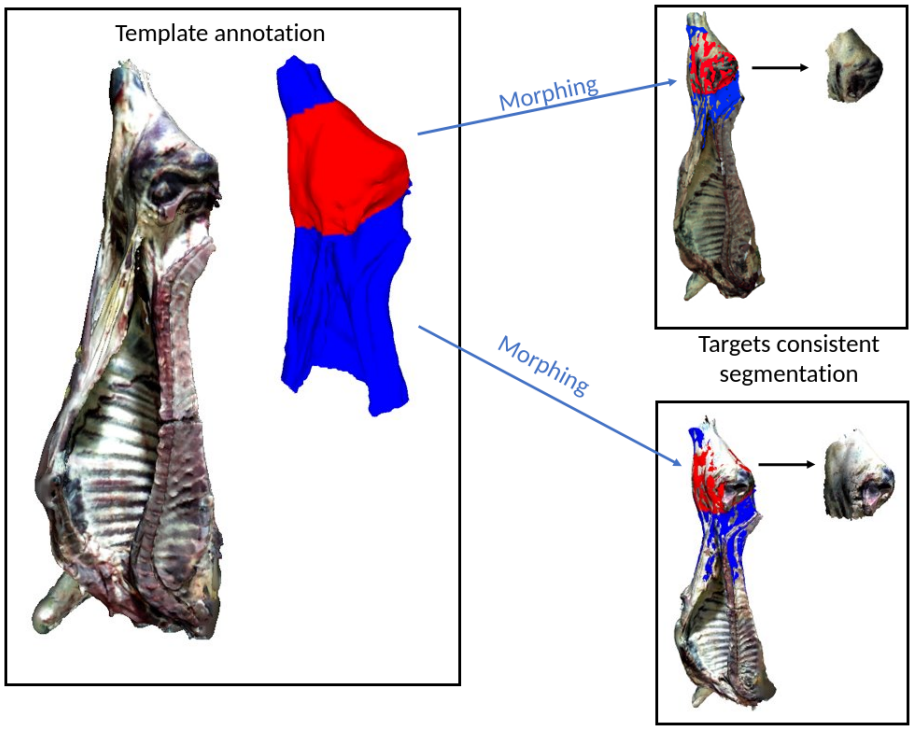

Figure 6: Illustration of the consistent segmentation procedure. A template is carefully annotated to select a specific area of the carcass side. This template is then morphed into all the other carcass sides (i.e., targets) and the annotation is then used to extract the region of interest consistently across all the dataset.

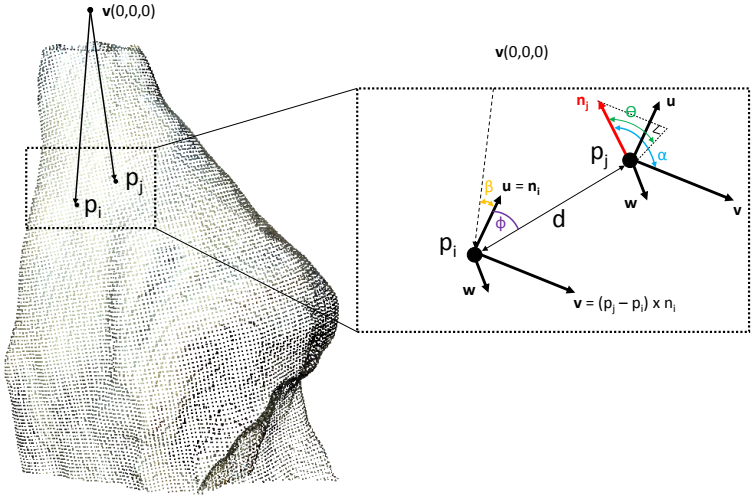

Figure 7: Darboux frame created using the pair of points p_i and p_j. The histogram of angles α, ϕ and θ between pairs of surface normals is referred to as a curvature descriptor.

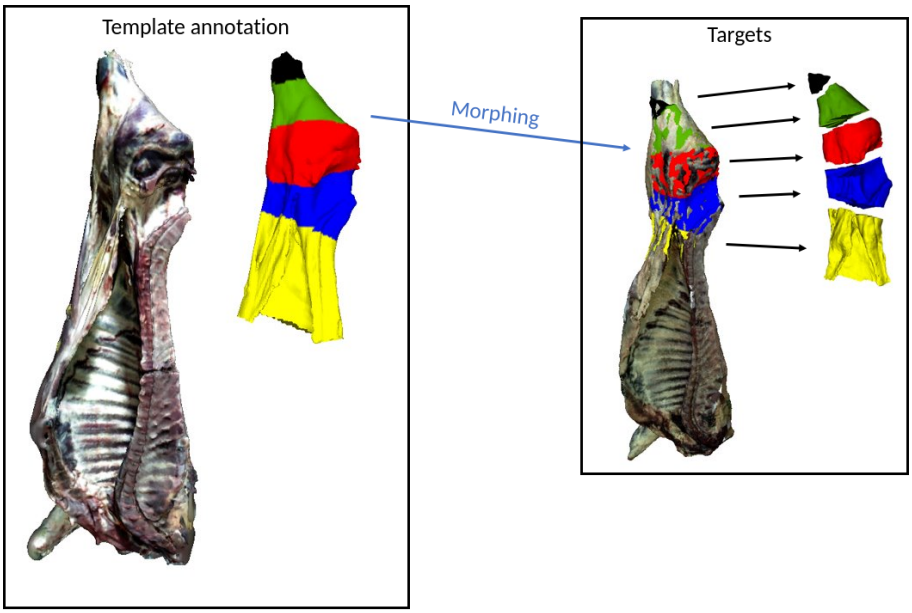

Figure 8: Illustration of the consistent volumetric computation procedure. Similarly to Figure 6, a template is annotated and morphed into the targets. This template is then cut virtually into pieces and the volume and surface area for each part is computed and aggregated into a signature.

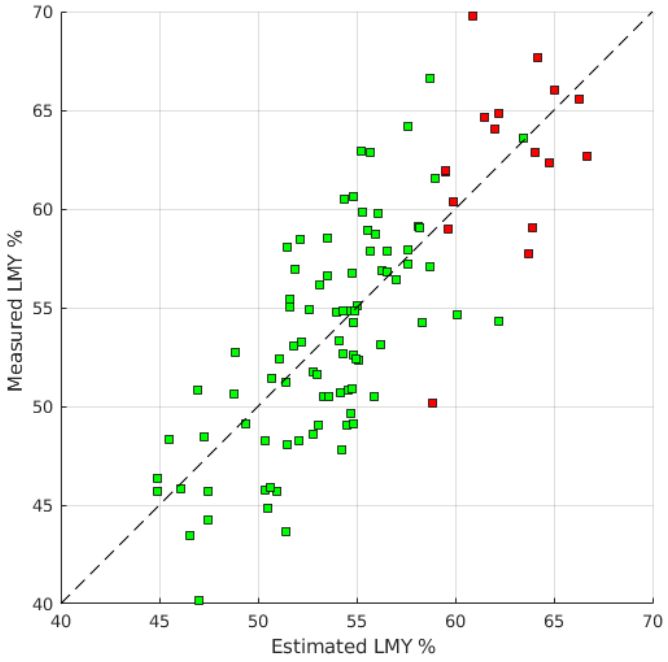

(a)

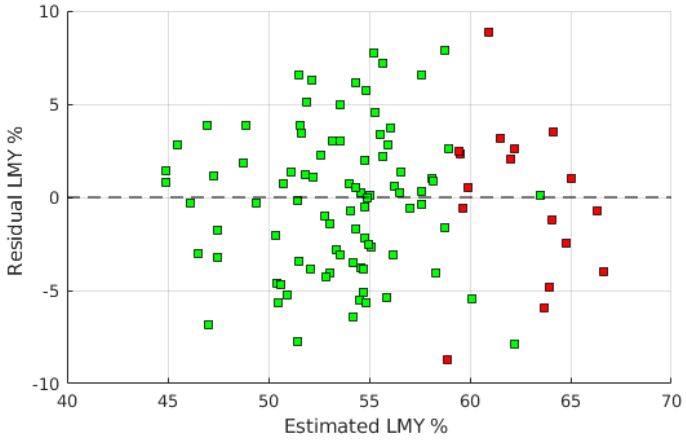

(b)

Figure 9: Plots showing (a) CT measured lean meat yield (LMY ,%) versus estimated LMY with a 1:1 (dashed line) and (b) residuals (measured – estimated) vs estimated LMY values, colours are indicative of carcasses from abattoir A (green) and B (red)

Table 1: Statistics of carcass traits (n = 119) divided into statistics for Abattoir A (n = 93) and Abattoir B (n = 26)

Trait	Range	Mean	Standard Deviation
	Abattoir A		
Left side HSCW (kg)	82 - 222	157.11	35.06
P8 (mm)	1 - 20	8.68	5.28
CT LMY (%)	40.16 - 66.58	53.33	5.31
	Abattoir B		
Left side HSCW (kg)	153 - 365	268.94	50.75
P8 (mm)	1 - 35	10.65	8.61
CT LMY (%)	50.17 - 70.63	63.43	4.93

Table 2: Analysis using Linear regression (n = 119), * was evaluated on a subset of (n = 26) carcass sides acquired at abattoir B.

Independent methods(s)	RMSE (%)	R^2
baseline - P8 + HSCW	6.90	0.01
segmentation by height - curvature descriptor	6.88	0.38
segmentation by height - curvature descriptor + P8 + HSCW	5.60	0.48
consistent segmentation - curvature descriptor	9.78	0.32
consistent segmentation - curvature descriptor + P8 + HSCW	5.20	0.62
*using feature reduction (GA) - curvature descriptor	4.75	0.53
*using feature reduction (GA) - curvature descriptor + P8 + HSCW	4.24	0.62

Table 3: Analysis using Gaussian process regressor (n = 119), * was evaluated on a subset of (n = 26) carcass sides acquired at abattoir B.

Independent methods(s)	RMSE (%)	R^2
baseline - P8 + HSCW	6.68	0.08
segmentation by height - curvature descriptor	4.57	0.60
segmentation by height - curvature descriptor + P8 + HSCW	4.40	0.62
consistent segmentation - curvature descriptor	4.34	0.62
consistent segmentation - curvature descriptor + P8 + HSCW	3.91	0.69
*using feature reduction (GA) - curvature descriptor	3.73	0.74
*using feature reduction (GA) - curvature descriptor + P8 + HSCW	3.66	0.69

Table 4: Feature descriptors comparison using a Gaussian process regressor. The volumetric features could not be computed on dataset A (as only the inner part of the carcass side was scanned), therefore, this comparison has been performed on n=27 from dataset B.

Independent methods(s)	RMSE (%)	R^2
consistent segmentation - curvature descriptor	4.37	0.33
consistent segmentation - Volume[1]	5.13	0.07